ELSEVIER

Journal of Nuclear Materials 257 (1998) 99–107

journal of nuclear materials

On the mechanism of Zircaloy cladding axial splits

V. Grigoriev *, B. Josefsson

Studsvik Material AB, SE-61182 Nyköping, Sweden

Received 16 February 1998; accepted 2 June 1998

Abstract

The macroscopically brittle axial splitting is treated as a process entirely accomplished by a plastic mechanism operating on a microscopic scale and is discussed in terms of the degree of plasticity and localisation of plasticity. The suggested mechanism involves hydrogen assisted localised shear (HALS) as a main factor of material deterioration. The reason and the driving force for the HALS is an in-plane shear (as for Mode II loading) existing at the tip of a crack loaded in Mode I (Opening). The HALS mechanism does not require brittle fracture of the hydrides and is only operable under certain combination of material strength, applied stresses, and temperature, needed for the local yielding at the crack tip. If the combination of those parameters results in the bulk yielding, the in-plane shear component is diminished and the delayed cracking is suppressed.

1. Introduction

The post defect degradation of LWR fuel rods occurs as a result of the oxidation and hydriding processes in the fuel-clad gap after the ingress of water. When describing the process of degradation, two cases have to be considered [1,2]: (1) a primary defect which does not propagate but which allows steam ingress and establishes conditions of oxygen starvation and secondary hydride damage elsewhere in the rod; and (2) a primary defect which is itself a sharp crack and which can be extended by a power ramp to a long axial split.

The morphology of long axial cracks indicates no measurable plastic deformation, which could be noticed as a wall thinning of the cladding, and the fracture surface is close to the axial–radial plane of the rod [1–3]. Such macro-brittle character of the failure led to the conclusion that the embrittlement of the cladding appears to be a pre-requisite for secondary degradation splits to occur [4,5].

Embrittlement of the cladding can be caused by irradiation damage, by hydriding, or by the formation of radial hydride platelets or massive hydride blisters [4,5]. It was also suggested that the embrittling effect of irradiation can be more pronounced in the material with smaller secondary phase particles (SPP) making current Zircaloy more susceptible to the cracking [2,5,6].

Nevertheless, the experimental evaluation of the resistance of Zircaloy cladding with different SPPs characteristics to the axial crack propagation did not reveal any tremendous embrittlement of irradiated material after $\sim 6 \times 10^{25}$ n/m^2 [7]. All irradiated cladding contained 100–200 wtppm of hydrogen and were quite ductile when tested at 573 K. Moreover, the hydrogen content in the range 25–800 wtppm did not influence the tensile ductility of irradiated cladding tested at 625 K after $\sim 10^{26}$ n/m^2 [8]. No appreciable embrittlement has been revealed in unirradiated cladding hydrided up to about 1000 wtppm and tested at 573–623 K by means of different techniques [7,9,10].

The apparent contradiction between a macroscopically brittle cracking during in-reactor axial split and ductile behaviour observed for similar material in short-term mechanical tests could be explained from the positions of the delayed hydride cracking (DHC) mechanism which is usually supposed to be the most plausible mechanism for the cases of splits developed from the primary defect [2,11]. Such explanation on the basis of DHC mechanism is debatable mainly for two reasons: (1) it is difficult to initiate DHC at temperatures of about

* Corresponding author. Tel.: +46-155 221 442; fax: +46-155 263 150; e-mail: vgrigoriev@studsvik.se.

0022-3115/98/$ – see front matter
PII: S0022-3115(98)00445-0

573 K [12] and (2) the brittle fracture of reoriented hydride under tensile stresses at 573–623 K can only be confirmed from the data obtained on the specimens prepared from a massive zirconium hydride piece [13,14]. In all other cases, when zirconium–zirconium hydride mixtures were tested at elevated temperatures, the long hydrides showed significant plasticity and tend to bend and flow with the ductile matrix without fracturing [15,16].

The purpose of the present work is to suggest an alternative explanation of the apparently brittle fracture of hydrided cladding at the temperatures well above the *brittle–ductile* transition in hydrided zirconium alloys. Such explanation would not be based on hydride brittleness, as the DHC mechanism is, and could describe the ability of the crack to run without any apparent ductile component. Thus, the problem of macroscopically brittle fracture of the cladding is treated as a process entirely accomplished by a plastic mechanism operating on a microscopic scale. From this point of view, the macroscopically brittle axial splitting of Zircaloy cladding is discussed in terms of the degree of plasticity and localisation of plasticity.

2. Fractographical observations

The existence of heavy shear at the tip of pre-fatigue crack in fracture toughness Zircaloy specimens had been noticed more than 20 years ago [17]. This shear area, situated between the fatigue crack and the area of fracture separation under the rising load, is a record, on the fracture surface, of crack tip blunting prior to crack extension.

The notched specimens of Zircaloy cladding, tested for characterisation of the post-irradiated fracture toughness [7], also showed a similar zone of shear fracture. All examined specimens independently of their structural conditions contained the extensive area of shear tearing (Fig. 1) extended up to the thinnest part of the cladding. The length of the shear area was 0.20–0.30 mm for irradiated specimens and 0.21 mm for unirradiated cold-worked (CW) specimen. The wall-thinning related to the bulk yielding at the notch tip was 24–27% for irradiated specimens and 36% for the CW specimen.

At higher magnifications the differences between two fracture modes, namely shear tearing for the crack blunting and dimpled rupture for the bulk yielding, can be easily distinguished (Fig. 2). The orientation of C-shaped tearing voids in the area of shear fracture indicates the existence of in-plane shear with shear stresses in the direction of crack propagation and with shear plane parallel to the notch plane. The existence of in-plane shear (as for Mode II loading) appears to be a common phenomenon for the crack tip conditions since the extensive areas of shear tearing were also observed in the fracture surfaces of Zircaloy and Zr–2,5Nb specimens after fracture toughness testing at elevated temperatures [18,19].

A similar in-plane shear component is also clearly distinguished in the specimen of irradiated Zircaloy cladding after delayed cracking at 573 K under sustained load [20]. The crack propagated from the left to the right (Fig. 3). The stable crack growth resulted in the in-plane shear fracture (Mode II) while the dimpled rupture occurred at the unstable crack growth path governed by Mode I loading. The transition from in-plane shear to the dimpled rupture appears to occur when the unstable

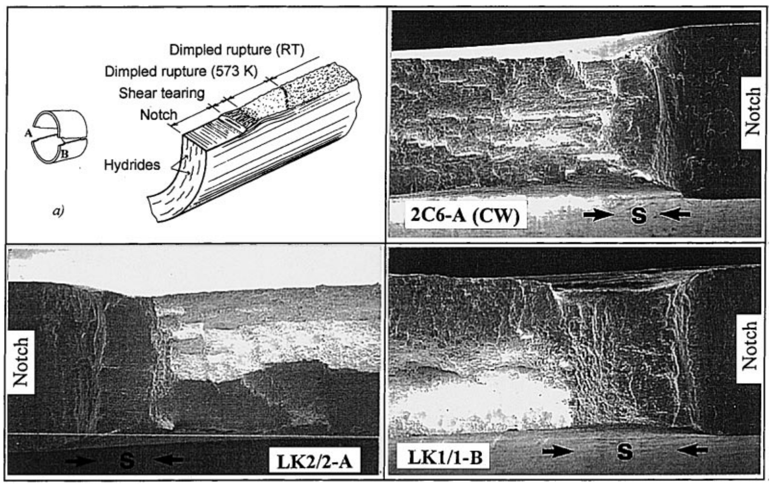

Fig. 1. (a) Typical macrotopography of Zircaloy cladding specimens after the PL tension test and (b–d) the fracture surface at the notch tip in unirradiated (2C6) and irradiated (LK1, LK2) Zircaloy-2 specimens. The area of in-plane shear fracture (shear tearing) is designated as *S*. For specimen designations see Ref. [7].

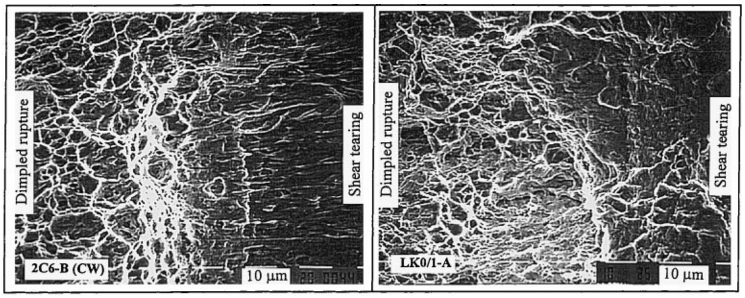

Fig. 2. The area of transition from shear tearing to dimpled rupture at the position of maximum thinning of Zircaloy cladding specimens: (a) unirradiated specimen 2C6-B (CW) and (b) irradiated specimen LK0/1-A. For specimen designations see Ref. [7].

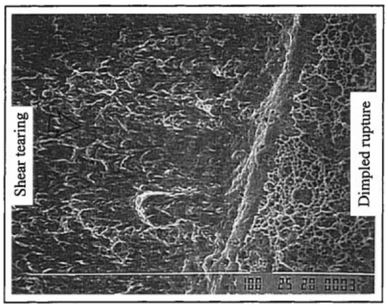

Fig. 3. The area of transition from shear tearing to dimpled rupture in the specimen of irradiated Zircaloy cladding after delayed cracking test under sustained load at 573 K [20].

crack growth is initiated in the specimen as a result of the overloading due to crack propagation (see Fig. 3). Again, the orientation of C-shaped tearing voids shows the direction of in-plane shear. In both cases (see Figs. 2 and 3) in-plane shear precedes dimpled rupture.

Thus, the general conclusions could be drawn from the fractographical observations: (a) the fracture processes at the crack tip occur under mixed tension-shear stress conditions (Mode I + Mode II), and (b) shear fracture (Mode II) dominates at the initial stages of the loading while the ductile rupture (Mode I) results from the bulk yielding.

3. In-plane shear at the crack tip

3.1. Shear strains at the crack tip

The obvious reason for additional stresses at the crack tip is the restraining of contractile deformations in the plastic zone. Such restraining occurs due to the surrounding material and in general case results in a triaxial stress state near the crack tip. For an axial crack in Zircaloy cladding the specimen thickness is too small to prevent the contraction in the radial (R) direction and $\sigma_R \approx 0$. Thus, the plastic zone should be under biaxial stress conditions with certain σ_A/σ_T ratio, where σ_T is tangential and σ_A is additional axial stress (Fig. 4(a)).

Since the material in the plastic zone aspires to contract its dimension in the axial direction but is prevented from that by the surrounding material, an in-plane shear component should arise at the boundary between the plastic zone and surrounding elastic body (Fig. 4(b)). Thus, two symmetrical areas of in-plane shear create the

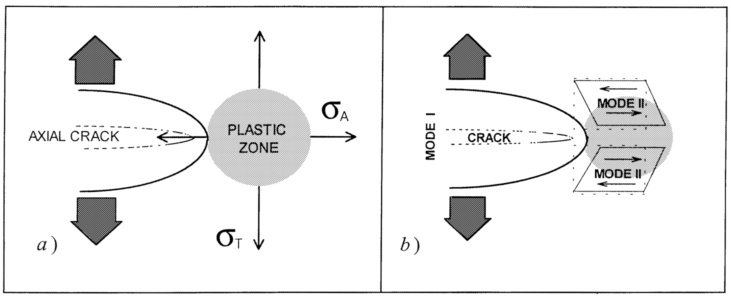

Fig. 4. Schematic of the stress/strain conditions at the tip of the loaded axial crack: (a) additional axial stress, σ_A, which is raised due to prevention of the axial contraction in the plastic zone, and (b) in-plane shear strain and stresses raised at the boundary of the plastic zone due to the distortion of the microvolumes at the crack tip. The distortion is mainly provided by the axial contraction in the plastic zone. The positions of the crack and the microvolumes at the crack tip before loading are shown by dashed lines.

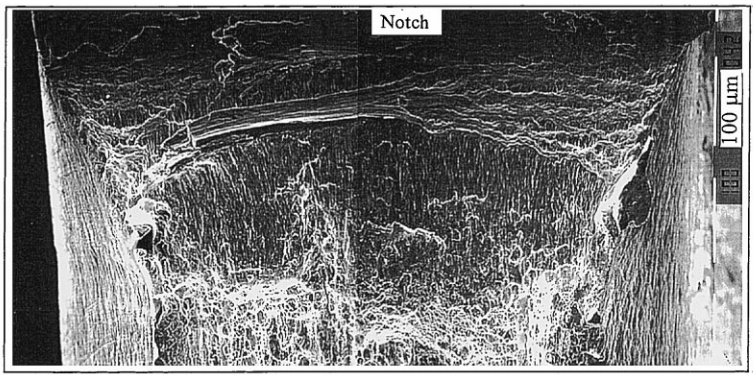

Fig. 5. Numerous nucleous of in-plane shear at the vicinity of the notch tip in Zircaloy cladding specimen after fracture toughness test.

features of the fracture surface characterised as tensile tearing [21], when elongated dimples on mating fracture surfaces are oriented in the same direction according to the crack propagation. Several nucleous of in-plane shear can be usually observed at the vicinity of the notch tip in Zircaloy cladding specimen after fracture toughness test (Fig. 5).

3.2. Yielding at the crack tip and in-plane shear

At least three cases have to be considered for the mixed tension-shear conditions at the crack tip. The classification can be based on the value of the normal (tangential) stress, σ_T, and related to the scale of material yielding at the crack tip.

In case 1, low σ_T cannot produce any yiedling and, thus, an in-plane shear is absent. At a moderate σ_T (Case 2) local yielding or a well-defined plastic zone is produced at the crack tip. The existence of a such zone results in appreciable in-plane shear (see Fig. 4(b)). At high σ_T (Case 3) the in-plane shear component disappears since the bulk yielding deletes the interaction between the plastic zone and surrounding elastic body.

The bulk yielding is accompanied by considerable wall thinning at the crack tip and a slant fracture or shear lips appears in the fracture surface depending on the specimen thickness and according to the orientation of maximum shear stress.

Depending on applied load all three cases can occur turn by turn in the same specimen during fracture toughness testing. As well as all three cases can be related to a classical crack velocity (da/dt) vs. stress intensity factor (K_I) curve (Fig. 6) with two distinct regions: (1) stable crack propagation (Stage II) and (2) unstable crack growth (Stage III). The fracture surface of the crack appears to be different at Stages II and III. The fracture governed by the local yielding just before the transition to Stage III results in the shear tearing

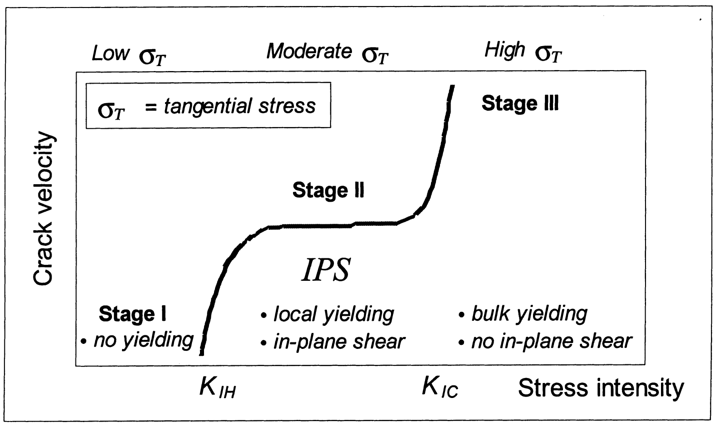

Fig. 6. The correlation between the stress/strain conditions at the crack tip and velocity of the crack. Stage II corresponds to the conditions of local yielding at the crack tip resulted in the in-plane shear (IPS) strains. The IPS is diminished when the bulk yielding occurs.

while the dimpled rupture is observed as a result of bulk yielding (see Figs. 2 and 3).

4. Shear strains and hydrogen effects

A number of experimental observations reveal close interrelationships between the matrix shear strain and hydride precipitation in zirconium materials. TEM investigations have shown that hydride precipitation in α-zirconium matrix is accompanied by large shear strains and by creation of shear dislocations [22]. The precipitation involves a shear transformation of the HCP lattice when a number of atomic layers undergo a shear along the basal plane. A similar shear process, which involves the generation of shear dislocations, was also observed for hydride precipitation in titanium [23].

4.1. Hydride reorientation

The shear stresses being applied to α-zirconium matrix promotes the precipitation of reoriented hydrides. Direct confirmation of the influence of shear stresses on hydride reoreientation was observed in notched Zi–2,5Nb specimens loaded in torsion (anti-plane shear or Mode III). In a few cases hydride reorientation under torsion was followed by intensive crack propagation [24].

Indirect confirming evidence that shear deformations promote hydride precipitation and growth can also be found in the description of hydride reorientation near the notch of the specimens stressed in tension. The reoriented hydrides were observed either in the intensively deformed shear zones near the notch root [25,26] or along the slip-lines [24].

4.2. Accelerated plastic flow

When hydride precipitation occurs in the matrix subjected to the shear stresses, the nucleation of additional shear dislocations can facilitate the material plastic flow. Such accelerating effect of hydride precipitation was observed in the experiments with zirconium specimens subjected to torsional shear stress in the creep regime [27]. The accelerated deformation was associated with hydride precipitation under applied stresses during electrolytic hydrogenation at room temperature. The hydrided specimen was then heated under torsion up to 593 K and later cooled down to room temperature. During the heating part of the cycle the hydrides were dissolved and all hydrogen came into solid solution. During cooling down the accelerated deformation was again observed when the hydride precipitation was triggered at the temperatures below the solubility limit.

The effectiveness of dislocation ‘production’ owing to hydride precipitation is illustrated in Fig. 7, which compiles the data on X-ray diffraction profile analysis of the dislocation density as a function of the hydride volume fraction in hydrided Zircaloy-4 [28] and as a function of the amount of cold working in zirconium alloys [29]. Thus, a hydrogen content of 600–700 wtppm can produce in recrystallised Zircaloy-4 a dislocation density similar to that in non-hydrided material after 40–60% of cold work.

No published data confirming the accelerating effect of hydride precipitation on material plastic flow under tension have been found. Perhaps, the effect is mainly pronounced under shear stresses. Nevertheless, two main effects of shear loading can be drawn out from experimental observations:

- shear strain promotes hydride reorientation;
- hydride precipitation facilitates the plastic shear in the matrix.

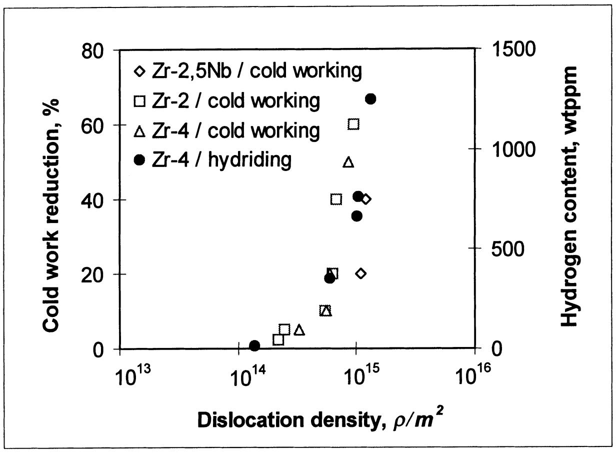

Fig. 7. The dislocation density in zirconium alloys as a function of hydrogen content and as a function of cold working [28,29].

5. Hydrogen assisted localised shear (HALS)

5.1. Mechanism of an axial split

All effects mentioned above can be applied to the case of hydride precipitation at the crack tip. Shear stresses at the crack tip distort microvolumes of the specimen (see Fig. 4(b)). In-plane shear strain, γ, can be defined as

$$\gamma \cong \tan \gamma = \delta l / l, \tag{1}$$

where the displacement, δl, is related to the axial contraction in the plastic zone (Fig. 8(a)).

In-plane shear strains promote hydride precipitation at the crack tip. Hydrides precipitate parallel to the crack plane, generate additional dislocations and, thus, decrease the stresses needed for plastic shear.

Besides the accelerating effect on plastic flow of the material, hydride precipitation can also facilitate the localisation of plastic shear along the hydride plane (Fig. 8(b)). It follows from the definition (1) that any decrease of the dimension l should drastically increase the accumulated shear deformation, γ'. The fracture at the crack tip should occur when the shear deformation γ', accommodated in the microvolume of the material, exceeds the threshold value, γ_{th}, needed for material fracture.

The in-plane shear component, γ, only exists at the crack tip when the local yielding is present (Fig. 9). Hydride precipitation introduces the localised shear, $\gamma' \gg \gamma$. For ductile material the localised shear deformation, γ', is still below the threshold value γ_{th}(D), and it is difficult to obtain the material fracture. For low-ductile material $\gamma' \geqslant \gamma_{th}$(LD) and crack propagation can be observed.

5.2. Localised deformation in irradiated Zircaloy

Mechanical behaviour of irradiated zirconium alloys is characterised by a highly inhomogeneous deformation

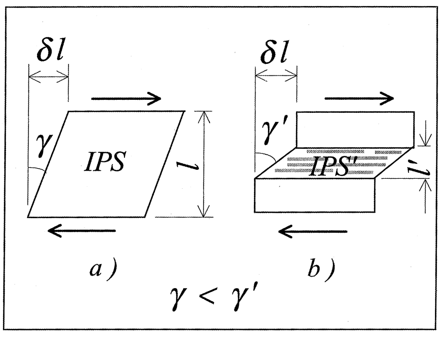

Fig. 8. The in-plane shear (IPS) strains at the crack tip: (a) the definition of shear strain $\gamma = \delta l/l$ and (b) the localised shear deformation $\gamma' \gg \gamma$ intensified due to HALS.

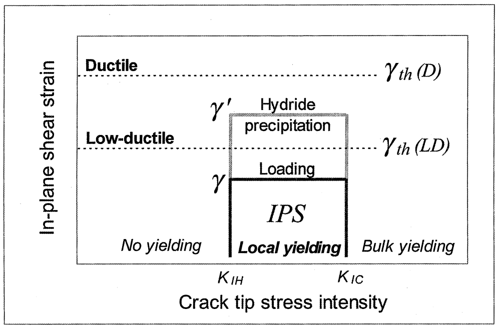

Fig. 9. Schematic showing the interrelationship between the in-plane shear (IPS) strains γ and γ' raised at the crack tip due to the HALS and the threshold values γ_{th} needed for material separation when the shear strength is reached. For ductile material $\gamma' < \gamma_{th}$(D) and shear fracture does not occur. For low-ductile material $\gamma' > \gamma_{th}$(LD) and the HALS may induce the apparently brittle fracture.

with intense shear bands confined to localised regions. Such concentrated shear deformation results from dislocation channelling and is suggested to depend on specimen geometry and stress state as well as on the availability of slip or deformation systems [30,31]. The ductility of irradiated Zircaloy at 600 K is limited by the localised deformation associated with dislocation channelling [32]. Although irradiation appears to facilitate localised deformation, the formation of dislocation channels, by itself, did not drastically reduce the ductility of Zircaloy [33]. In the absence of hydrogen, the material within a dislocation channel work hardened and a new channel was formed [31]. Thus, both irradiation and hydrogen have synergetic effects promoting the localisation of plastic flow in the material.

In the case of an axial crack in Zircaloy the direction of in-plane shear is predominantly oriented along the basal planes. According to the HALS mechanism this results in the most favourable conditions for material deterioration at the crack tip, since in irradiated Zircaloy both the hydride habit plane and the plane of dislocation channelling have similar orientation close to the basal plane [30,34].

The in-plane shear due to only external load cannot solely break the interatomic bonds across the shear plane. The additional power comes from the hydrogen–hydrogen interaction, which is the driving force for the martensitic phase transformation during hydride precipitation. This power induces additional shear distortion across the habit plane. The synergistic shear effects resulted from the external load and hydride precipitation and accommodated by means of the basal slip channelling may highly localise the in-plane shear at the crack tip and, thus, facilitate the breaking of atomic bonds across the basal planes. Depending on the degree of material plasticity and localisation of plasticity, the resulted fracture surface might contain different fractographical features including those similar to the quasi-cleavage facets.

A more detailed discussion of the fracture mechanisms apparently should take into account that the fracture processes at the crack tip occur under mixed tension-shear stresses. Several specific factors co-exist simultaneously at the moment of hydride precipitation: (1) thin layer of the material with explosively increased mobility of the atoms; (2) shear stresses oriented parallel to that layer; (3) tensile stresses oriented perpendicular to that layer. Perhaps, the description of the fracture process cannot be simply based on the threshold stress or strain criteria but should include a thermodynamic balance of mechanical, chemical, and thermal energies combined to exceed the binding energy of zirconium atoms.

It cannot be ruled out that at elevated temperature the hydrides themselves are more susceptible to the shear fracture than to the fracture under tension, especially when they are embedded in the ductile matrix. In this case the fracture at the crack tip could occur not because of breaking of interatomic zirconium bonds in the matrix but as a result of shear deformation accumulated in precipitating hydrides. In any case, the process repeats itself and, owing to the crack plane symmetry, may result in the crack propagation by means of switching from one plane of hydride platelets to another with the distance between planes being of the order of the crack-opening displacement (see Fig. 4(b)). Such step-wise topography of the crack surface is typical for the failed Zircaloy cladding [2,3]. Similar type of crack propagation has earlier been described for delayed cracking in Zr–2,5Nb [35].

Independent of whether the fracture occurs due to breaking of interatomic zirconium bonds or as a result of shear fracture of precipitating hydride, the hydrided material should be more sensitive to the shear loading than to tension. Such behaviour has really been observed for unirradiated hydrided Zircaloy cladding ($\sim$500 wtppm). Both hydrided and as-received cladding showed practically the same reduction of area when smooth specimens were tested at 573 K under uniaxial tension in the axial and circumferential directions [36]. However, when the notched specimens of the same cladding were tested at 573 K under axial shear along the axial–radial plane, hydrided material showed only half of the fracture deformation obtained for as-received cladding [37]. Indirect confirmation of higher susceptibility of hydrided Zircaloy-4 cladding to the shear fracture can also be drawn out from the observation that the addition of 700 wtppm hydrogen had no effect on uniform elongation of smooth specimen but resulted in a considerable reduction of localised (necking) deformation which involved the development of shear bands [30].

5.3. Factors affecting the axial splits

The suggested mechanism of Zircaloy cladding axial splits involves hydrogen assisted localised shear as a main factor of material deterioration at the crack tip. The reason and the driving force for the HALS is an in-plane shear (as for Mode II loading) which arises at the tip of a crack loaded in Mode I (Opening).

A shear component only exists when the plastic zone at the crack tip is surrounded by an elastic body. Thus, the stresses should be high enough to produce a well-defined plastic zone at the crack tip with a pronounced shear component. On the other hand, the stresses should not be too high, otherwise the bulk yielding at the crack tip diminishes the in-plane shear. This requirement is provided by the combination of test temperature, applied load, and material strength. As soon as any of these parameters promote bulk yielding at the crack tip, there is no reason for in-plane shear to be present. The inhibiting effect of the bulk yielding on crack propagation has been observed in hydrided zirconium materials [12].

Another important item is the role of hydride precipitation. In the HALS mechanism the hydride precipitation under tension-shear stresses is a key moment of material deterioration at the crack tip. The collective movement of zirconium atoms, caused by the hydrogen-hydrogen interaction and oriented in the same direction as external forces act, might result in heavy deterioration of the material already at the moment of hydride precipitation. Continuous precipitation of reoriented hydrides at the crack tip results in crack propagation. It could mean that the cladding should be less susceptible to the axial splits when the hydride reorientation under mixed shear-tension stresses at the crack tip is scarced. Further, the higher the ductility of hydrided cladding under shear loading, the larger deformation can be accumulated in the material before separation, and, so, the less susceptible is the cladding to the axial splits. Thus, any factor which decreases the ductility of the cladding should facilitate the axial splits.

Among the factors, which affect the ductility, the irradiation hardening and stress-state biaxiality appear to be the most considerable. The saturation of the cladding hardening can be mainly achieved after $\sim 10^{25}$ n/m^2. But, as it has already been mentioned, the irradiation itself does not drastically reduce the ductility of Zircaloy. As to the stress-state, the worst possible case is equal biaxial tension, such as would be the case if there were a very strong pellet-cladding bond or friction during the fuel expansion in a power ramp.

In the case of an axial crack, several factors appear to be simultaneously present and superimposed at the crack tip leading to the apparently brittle fracture: (1) *biaxial tensile stresses* owing to fuel pellet thermal expansion; (2) *biaxial tensile stresses* as a crack tip effect; (3) *in-plane shear* due to axial contraction in the plastic zone; (4) *in-plane shear* as a result of hydride precipitation; (5) *localisation of the in-plane shear* resulted from the hydride precipitation; (6) *localisation of the in-plane shear* due to basal slip channelling; (7) *facilitated dislocation channelling* due to hydride precipitation; (8) *low strain hardening* inside the channels owing to hydrogen presence. As a result of such combination, the apparently brittle fracture of intrinsically ductile cladding might occur.

6. Conclusions

A mechanism is suggested to explain Zircaloy cladding splits as a process entirely accomplished by a plastic mechanism operating on a microscopic scale. Qualitative description of the mechanism is based on the available observations of mechanical behaviour of hydrided zirconium materials under shear loading.

The suggested mechanism involves HALS as a main factor of material deterioration which results in the delayed cracking. The reason and the driving force for the HALS is an in-plane shear (as for Mode II loading) existing at the tip of a crack loaded in Mode I (Opening). Due to the texture of the cladding Mode II is the most pronounced for the axial crack orientation.

The HALS mechanism does not require brittle fracture of the hydrides and is only operable under certain combinations of material strength, applied stresses, and temperature provided that the local yielding at the crack tip is present. If the combination of those parameters results in the bulk yielding at the crack tip, the in-plane shear component is diminished and the delayed cracking is suppressed.

Shear distorsion from the hydride precipitation is superimposed on the in-plane shear caused by the external load applied to the crack. In irradiated cladding the synergetic shear effects can be additionally localised due to the basal slip channelling. Such localisation under mixed tension-shear stresses might result in the apparently brittle fracture of intrinsically ductile cladding.

Acknowledgements

The main ideas of this work were developed under the projects jointly sponsored by Vattenfall AB, OKG Aktiebolag, Barsebäck Kraft AB, ABB Atom AB, and Studsvik AB whose support is gratefully acknowledged. The authors are grateful to Dr Pål Efsing for making the micrograph in Fig. 3 available.

References

[1] J.S. Armijo, in: Proceedings of the International Topical Meeting on LWR Fuel Performance, 1994, p. 410.
[2] K. Lin, C.S. Chung, J.J. Yeh, J.H. Chen, S.S. Chu, L.F. Lin, in: Proceedings of the International Topical Meeting on LWR Fuel Performance, 1994, p. 377.
[3] D. Schrire, B. Grapengiesser, L. Hallstadius, L. Lundholm, G. Rönnberg, G. Lysell, Å. Jonsson, G. Frenning, in: Proceedings of the International Topical Meeting on LWR Fuel Performance (1994) p. 398.
[4] R.L. Yang, O. Ozer, S.K. Yagnik, B. Cheng, in: Proceedings of the International Topical Meeting on LWR Fuel Performance, 1994, p. 435.
[5] R.O. Montgomery, Y.R. Rashid, O. Ozer, in: Proceedings of the International Topical Meeting on LWR Fuel Performance, 1994 p. 447.
[6] C.D. Williams, M.O. Marlowe, R.B. Adamson, S.B. Wisner, R.A. Rand, J.S. Armijo, in: Proceedings of the 11th International Symposium on Zirconium in the Nuclear Industry, ASTM STP 1295, 1996, p. 676.
[7] V. Grigoriev, B. Josefsson, B. Rosborg, in: Proceedings of the 11th International Symposium on Zirconium in the Nuclear Industry, ASTM STP 1295, 1996, p. 431.
[8] S.B. Wisner, R.B. Adamson, in: Proceedings of the Enlarged Halden Programme Group Meeting, vol. 1, 1996, HPR-347/12.
[9] J.B. Bai, C. Priol, D. Francois, Metall. Mater. Trans. 25A (1994) 1185.
[10] S. Suzuki, K. Murakami, T. Takahashi, in: Proceedings of the International Topical Meeting on LWR Fuel Performance, 1994, p. 352.
[11] L. Lundholm, P. Efsing, G. Lysell, D. Schrire, in: Proceedings of the Enlarged Halden Program Group Meeting, vol. II, 1993, HPR-343.
[12] R.R. Smith, R.L. Eadie, Scripta Metall. 22 (1988) 833.
[13] K.G. Barraclough, C.J. Beevers, J. Mater. Sci. 4 (1969) 518.
[14] L.A. Simpson, C.D. Cann, J. Nucl. Mater. 87 (1979) 303.
[15] R. Choubey, M.P. Puls, Metall. Mater. Trans. 25A (1994) 993.
[16] S. Arsene, J.B. Bai, Ecole Centrale Paris, Laboratoire de Mecanique, private communication.
[17] T.J. Walker, J.N. Kass, in: Proceedings of the Symposium on Zirconium in Nuclear Applications, ASTM STP 551, 1974, p. 328.
[18] L.A. Simpson, C.K. Chow, in: Proceedings of the Seventh International Symposium on Zirconium in the Nuclear Industry, ASTM STP 939, 1987, p. 579.
[19] P.H. Davies, R.R. Hosbons, M. Griffiths, C.K. Chow, in: Proceedings of the Tenth International Symposium on Zirconium in the Nuclear Industry, ASTM STP 1245, 1994, p. 135.
[20] P. Efsing, K. Pettersson, in: Proceedings of the 12th International Symposium on Zirconium in the Nuclear Industry, ASTM STP 1354, to be published.
[21] C.D. Beachem, Trans. ASM 56 (1963) 318.
[22] G.J.C. Carpenter, Acta Metall. 26 (1978) 1225.
[23] H.Z. Xiao, Scripta Metall. 27 (1992) 571.
[24] M.P. Puls, A.J. Rogowsky, in: Proceedings of the NATO Advanced Research Institute on Atomistics of Fracture, 1981, p. 789.

[25] F.H. Huang, W.J. Mills, Metall. Trans. 22A (1991) 2049.
[26] C.J. Simpson, O.A. Kupcis, D.V. Leemans, in: Proceedings of the Third International Symposium on Zirconium in the Nuclear Industry, ASTM STP 633, 1977, p. 630.
[27] L.V. Spivak, N.Y. Skryabina, Fiz Metal Metalloved, 81 (1996) 165 (in Russian).
[28] J.B. Bai, J. Mater. Sci. Lett. 12 (1993) 677.
[29] P. Merle, K. Loucif, L. Adami, R. Borrelly, J. Nucl. Mater. 208 (1994) 135.
[30] A.M. Garde, in: Proceedings of the Eighth International Symposium on Zirconium in the Nuclear Industry, ASTM STP 1023, 1989, p. 548.
[31] D. Lee, R.B. Adamson, in: Proceedings of the Third International Symposium on Zirconium in the Nuclear Industry, ASTM STP 633, 1977, p. 385.
[32] A.M. Garde, G.P. Smith, R.C. Pirek, in: Proceedings of the 11th Symposium on Zirconium in the Nuclear Industry, ASTM STP 1295, 1996, p. 407.
[33] P. Morize, J. Baicry, J.P. Mardon, in: Proceedings of the Seventh International Symposium on Zirconium in the Nuclear Industry, ASTM STP 939, 1987, p. 101.
[34] K. Pettersson, J. Nucl. Mater. 105 (1982) 341.
[35] L.A. Simpson, in: Proceedings of the Third International Conference on Mechanical Behaviour of Materials, vol. 2, 1979, p. 445.
[36] V. Grigoriev, K. Pettersson, S. Andersson, in: Proceedings of the 12th International Symposium on Zirconium in the Nuclear Industry, ASTM STP 1354, to be published.
[37] V. Grigoriev, A. Moberg, 1997, unpublished results.